Physically-constrained multi-frame blind deconvolution

Roberto Baena Gallé[1,2,3], Szymon Gladysz[3], Laurent Mugnier[4], Rao Gudimetla[5], Robert L. Johnson[5], Lee Kann[5]

[1]*University of Barcelona, c\Marti I Franqués 1, 08025 Barcelona, Spain*
[2]*Royal Academy of Sciences and Arts of Barcelona, Rambla dels Estudis 115, 08002 Barcelona, Spain*
[3]*Fraunhofer Institute of Optronics, System Technologies and Image Exploitation, Gutleuthausstr. 1, 76275 Ettlingen, Germany*
[4] *ONERA/DOTA (Département d'Optique Théorique et Appliquée), B.P. 72, 92322 Châtillon cedex, France*
[5]*Air Force Research Laboratory, Directed Energy Directorate, Kirtland AFB, NM, USA*

Author e-mail address: rbaena@am.ub.es

Abstract: We propose a set of statistical constraints for the problem of imaging through atmospheric turbulence. The constraints, in the form of probability density functions or log-likelihoods, describe image variability in three domains: focal plane, pupil plane or Fourier plane. The constraints are incorporated in the maximum *a posteriori* framework.

OCIS codes: (110.0115) Imaging through turbulent media, (100.1455) Blind deconvolution

1. Introduction

Solutions to recovery of high-resolution images when observing through atmospheric turbulence usually fall into the software ("post-processing") or the hardware (adaptive optics, interferometry) category or the combination of both. Even with very expensive adaptive optics (AO) systems it is necessary to use deconvolution (image reconstruction) to remove image blurring completely [1,2].

Successful restoration of images degraded by atmospheric turbulence was first achieved using the co-called speckle imaging techniques [3]. Speckle imaging works because average short-exposure power spectrum has non-negligible spectral content up to the telescope's diffraction limit D/λ [4]. On the other hand, for long exposures average optical transfer function (OTF) quickly drops to values below the noise limit above the cut-off r_0/λ. No information can be recovered from the part of the spectrum where signal-to-noise ratio (SNR) falls below unity. It is this SNR cutoff that actually determines available resolution, with or without deconvolution, and the SNR cutoff is nearly always short of the diffraction cutoff [5]. Therefore, non-regularized deconvolution of long-exposure images, taken without AO, rarely results in reliable amplification of the high-frequency content.

Multi-frame blind deconvolution (MFBD) [6-8] is an image reconstruction method relying on the availability of several images of an object. In addition, many of the MFBD algorithms rely on short exposures for the reason stated above. The multiplicity of image frames acts as an implied constraint because the object is common to every image, while noise and turbulence fluctuations vary randomly between frames [5]. Even with this advantage, MFBD can get easily trapped in local minima [9]. We are studying approaches to alleviating this problem.

2. Motivation

Regularization is the most popular approach to balancing resolution enhancement and amplification of noise. Early termination of the iterative process or an additional spectral filter can be thought of as simple regularization methods [5]. In our work, we rely on the explicit inclusion of all possible priors, whether connected to the object or the PSFs, which is the maximum *a posteriori* (MAP) framework. In this approach one finds estimates for the object $\mathbf{o}$ and the PSFs $\mathbf{h}$ which jointly maximize the data-fitting term, $p(\mathbf{i} \mid \mathbf{o},\mathbf{h})$ – where $\mathbf{i}$ is the data – and the prior probability of the object, $p(\mathbf{o})$, together with the prior probability of the PSFs, $p(\mathbf{h})$:

$$[\hat{\mathbf{o}},\hat{\mathbf{h}}] = \arg\max_{\mathbf{o},\,\mathbf{h}} p(\mathbf{o},\mathbf{h}\mid\mathbf{i}) = \arg\max_{\mathbf{o},\,\mathbf{h}} p(\mathbf{i}\mid\mathbf{o},\mathbf{h}) \times p(\mathbf{o}) \times p(\mathbf{h}) \tag{1}$$

Since probability density function $p(\mathbf{o})$ is in general not known, solutions in the form of functions with desirable mathematical properties (e.g. noise suppression, edge enhancement) are often used. As these *ad hoc* formulas are not real probability density functions (PDFs), regularization parameters must be used to balance their influence on the cost function in Equation (1). Often these parameters have to be chosen manually [1,8]. Apart from the problem of choosing the right value for the parameters, the mere form of the prior (e.g. an object's power spectral density [10]) could be applicable only to a limited class of real objects.

For these reasons we focus on PSF statistics. This part of Equation (1) was almost always removed from the MAP approach [7,10]. Formulas for wavefront statistics and, by extension, for short-exposure PSF statistics have been used in the field of wavefront reconstruction and deconvolution from wavefront sensing [11] but not in the field of image restoration. The few papers which deal with the PSF prior do so for the case of long exposures [1,12].

Here we present ideas on how to incorporate the body of knowledge about turbulence-induced statistics of various quantities like intensity or Fourier components into the MAP framework.

3. Equations

For the data-fidelity term in Equation (1) we use the standard maximum-likelihood expression under the assumption of stationary Gaussian noise. The PSF constraints, which are the focus of this communication, can be formulated in three domains: image, pupil or Fourier-frequency space. We present the formulas in separate sections. In the equations *K* is the number of speckle frames and *N* and *M* are the numbers of pixels in x and y directions.

Image plane

In the focal plane of an optical system speckle intensity is known to be well approximated by the exponential PDF [4]. Joint statistics for the entire image ensemble, under the assumption of independence, are:

$$p(\mathbf{h}) = \prod_{k}^{K}\prod_{x}^{N}\prod_{y}^{M} \frac{1}{\overline{h(x,y)}} e^{-\frac{h(k,x,y)}{\overline{h(x,y)}}} \tag{2}$$

The mean PSF $\overline{h(x,y)}$ needs to be estimated directly from the data to satisfy the "no reference" goal of the project. This is done using the "Fourier contrast" method [13]. For temporally-integrated speckle gamma PDF could be used [4].

Pupil plane

Wavefront phase can be decomposed into Zernike polynomials [11]. This allows one to work with fewer variables. Treating vectors of Zernike coefficients as random processes we arrive at the following PDF:

$$p(\phi) = \frac{1}{(2\pi)^{KL/2}|C|^{K/2}} \prod_{k}^{K} \exp\left(-\frac{1}{2}\phi_k^T C^{-1} \phi_k\right) \tag{3}$$

where *C* is the covariance matrix of the first *L* Zernike coefficients, |C| is the determinant of the covariance matrix, and ϕ_k means a vector of Zernike coefficients for image number *k*.

Fourier plane

Statistics of the squared modulus of the short-exposure OTF can be well approximated by PDF of short-exposure intensity [4,13]. Therefore, it is conceivable that the gamma-based, Strehl-ratio PDF [14] could explain the statistics of $|H(u,v)|^2$ across the entire frequency range [13]. Alternatively, one could constrain the modulation transfer function (MTF) using a similarly-derived PDF:

$$p(|\mathbf{H}|) = \prod_{k}^{K}\prod_{u}^{N}\prod_{v}^{M} 2\frac{\left(\frac{-2\ln(|H(k,u,v)|)}{\theta}\right)^{k-1} |H(k,u,v)|^{\frac{2-\theta}{\theta}}}{\Gamma(k)\theta} \tag{4}$$

where parameters $k = (m(u,v)-1)/2$ and $\theta = 2D_\phi(u,v)/m(u,v)$ are both functions of the spatial frequency through the number of OTF cells $m(u,v)$ and the phase structure function $D_\phi(u,v)$ [13]. Alternatively, real and imaginary parts of the OTF can be assumed to follow joint Gaussian PDF with the following moments:

$$\overline{\Re} = e^{-\frac{D_\phi(u,v)}{2}}, \quad \overline{\Im} = 0, \quad \sigma_\Re^2 = \frac{1}{2m(u,v)}\left[1 + e^{-2D_\phi(u,v)} - 2e^{-D_\phi(u,v)}\right], \quad \sigma_\Im^2 = \frac{1}{2m(u,v)}\left[1 - e^{-2D_\phi(u,v)}\right] \tag{5}$$

In Figure 1 this model is tested against the SOR data described in the next section.

4. Preliminary results

We present results based on the focal-plane constraint, Equation (2). The model PDFs were converted to negative log-likelihoods and, together with analytic gradients, inserted into the conjugate-gradient optimizer [15]. I-band (850nm) observations of the bright single star HR2219 have been obtained with the 3.5m telescope at the Starfire Optical Range with AO switched off (tip/tilt on). Thousand frames were recorded, with exposure time set to 10ms.

Two objects have been used to generate these preliminary results. The first one corresponds to a circle with two lobes on the top. All the pixels were set to the same value of 252. The second one is showing the Hubble Space Telescope (HST), its dynamic range is between 30 and 250 a.u. These two objects were convolved with the first 50 SOR frames. White noise with standard deviation equal to 1 was then added.

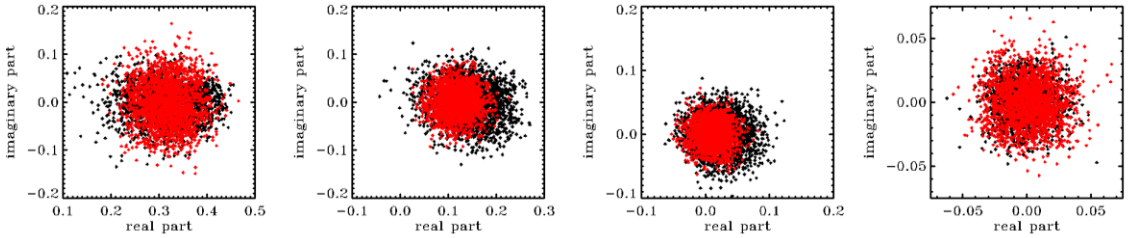

Fig. 1. Distributions of the real and imaginary parts of the OTF: empirical – based on the speckle frames from SOR (black) and modeled, using random numbers drawn from joint Gaussian PDF with moments given by Equation (5), in red. Pupil-plane distances are: $0.5r_0$, $1r_0$, $1.5r_0$, $3r_0$.

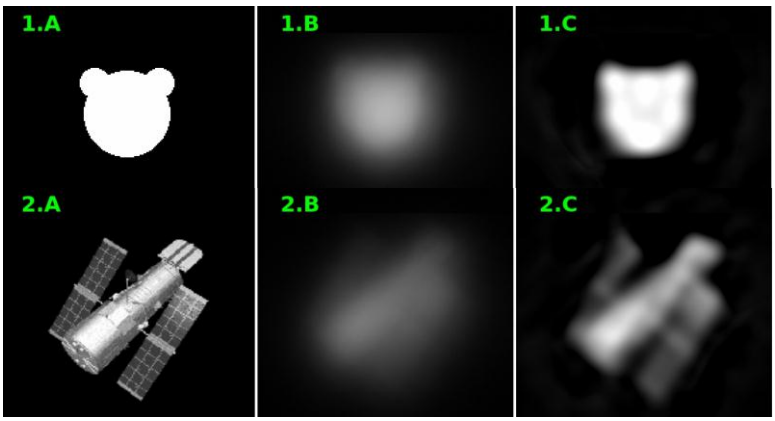

Fig. 2. Column A: original objects. Column B: frame number 1 of the blurred and noisy simulations. Column C: reconstructions: 1.C – 100 iterations, 2.C – 200 iterations. Images are represented on linear scale from 0 to 250.

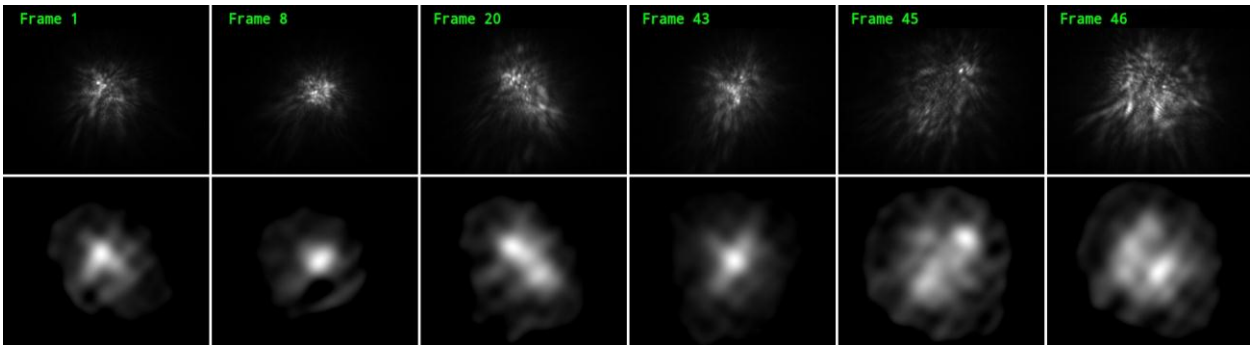

Fig. 3. Top row: some of the original PSFs (D/r_0 = 34 from the "Fourier contrast" method [13]). Bottom row: the corresponding reconstructions. Note how reconstructed PSFs, based on the HST dataset, try to follow the original shapes, elongations and maximum peak positions.

ACKNOWLEDGEMENTS: Effort sponsored by U.S. Air Force Office of Scientific Research, Air Force Material Command, under grant FA8655-12-1-2115, and the Spanish Ministry of Science under grant AyA-2008-01125. The U.S. Government is authorized to reproduce and distribute reprints for Governmental purpose notwithstanding any copyright notation thereon.

5. References

[1] L. M. Mugnier, T. Fusco, and J.-M. Conan, "MISTRAL: a myopic edge-preserving image restoration method, with application to astronomical adaptive-optics-corrected long-exposure images," J. Opt. Soc. Am. A 21, 1841-1854 (2004).
[2] R. Baena Gallé, J. Núñez, and S. Gladysz, "Extended object reconstruction in adaptive-optics imaging: the multiresolution approach," submitted to Astronomy & Astrophysics.
[3] A. Labeyrie, "Attainment of diffraction-limited resolution in large telescopes by Fourier-analyzing speckle patterns in star images," Astronomy & Astrophysics 6, 85-87 (1970).
[4] J. W. Goodman, "Speckle phenomena in optics: theory and applications," (Roberts & Company, 2006).
[5] D. W. Tyler, "Deconvolution of adaptive optics image data," Proceedings of the Center for Adaptive Optics, (2001).
[6] T. J. Schulz, "Multiframe blind deconvolution of astronomical images," J. Opt. Soc. Am. A 10, 1064-1073 (1993).
[7] D. G. Sheppard, B. R. Hunt, and M. W. Marcellin, "Iterative multiframe superresolution algorithms for atmospheric-turbulence-degraded imagery," J. Opt. Soc. Am. A 15, 978-992 (1998).
[8] C. L. Matson, K. Borelli, S. Jefferies, C. C. Beckner, Jr., E. K. Hege, and M. Lloyd-Hart, "Fast and optimal multiframe blind deconvolution algorithm for high-resolution ground-based imaging of space objects," Appl. Opt. 48, A75-A92 (2009).
[9] J. Nagy and V. Mejia-Bustamante, "MFBD and the local minimum trap," Proceedings of the AMOS Conference, 2009, Ed.: S. Ryan, The Maui Economic Development Board, p.E10
[10] L. Blanco and L. M. Mugnier, "Marginal blind deconvolution of adaptive optics retinal images," Opt. Express 19, 23227-23239 (2011).
[11] L. M. Mugnier, C. Robert, J.-M. Conan, V. Michau, and S. Salem, "Myopic deconvolution from wave-front sensing," J. Opt. Soc. Am. A 18, 862-872 (2001).
[12] A. MacDonald, S. C. Cain, and E. E. Armstrong, "Maximum a posteriori image and seeing condition estimation from partially coherent two-dimensional light detection and ranging images," Opt. Eng. 45, 086201-1-13 (2006).
[13] S. Gladysz, R. Baena Gallé, R. Johnson, and L. Kann, "Image reconstruction of extended objects: demonstration with the Starfire Optical Range 3.5m telescope," Proceedings of SPIE, Volume 8535, 85350M-1-13 (2012).
[14] S. Gladysz, J. C. Christou, L. W. Bradford, and L. C. Roberts, Jr., "Temporal variability and statistics of the Strehl ratio in adaptive-optics images," PASP 120,1132-1143 (2008).
[15] E. Thiebaut, "Optimization issues in blind deconvolution algorithms," in Astronomical Data Analysis II, SPIE Vol. 4847, 174-183 (2002).